Bulletin of Earth Sciences of Thailand

Quantifying crustal deformation caused by the Cianjur tectonic earthquakes magnitude 5.6 through DInSAR and GNSS technology

Muhammad Hanif* and Sakpod Tongleamnak
[1] Geoinformatics, Department of Computer Science, College of Computing, Khon Kaen University, 40002. Thailand

*Corresponding author e-mail: muhammad.h@kkumail.com

Abstract

Indonesia, an archipelagic country situated within the volatile Ring of Fire and the convergence of multiple tectonic plates, frequently experiences seismic activity. These earthquakes have led to alterations in the Earth's surface layers and even damage to the land. The Cianjur earthquake, which occurred on November 21, 2022, was a shallow crustal tectonic earthquake of the mainshock variety, followed by a series of aftershocks. The objective of this research is to conduct deformation mapping before and after the Cianjur Magnitude 5.6 earthquake. The research employs remote sensing technology, specifically differential interferometric synthetic aperture radar (DInSAR), in conjunction with global navigation satellite system (GNSS) analysis techniques. The results have yielded valuable insights into the spatial distribution of vertical tectonic deformation through DInSAR and GNSS analysis, revealing that the co-seismic deformation reached a maximum value of 5.87 cm, concentrated in the Cugenang sub-district. In contrast, GNSS station data recorded co-seismic deformation of 4.6 cm and horizontal deformation of approximately ±12 cm, directed southeastward. These findings indicate that aftershocks had a more significant impact on deformation in the Cianjur region, particularly around the Cugenang fault area. Variations in the source of the main earthquake and subsequent aftershocks substantially influenced deformation patterns and the direction of horizontal deformation.

Keywords: crustal deformation, geohazard, synthetic aperture radar

1. Introduction

Earthquakes are a common natural disaster in Indonesia. The tectonic activity leading to an earthquake typically follows a sequence, starting with foreshocks, which are smaller earthquakes that precede the main event. Subsequently, a mainshock occurs, characterized by the highest magnitude and significant impacts on geological and environmental conditions in the affected area. Aftershocks, which continue to occur after the main earthquake, can persist for an extended period, although their frequency and magnitude generally decrease over time. On November 21, 2022, a tectonic earthquake struck Sukabumi, West Java, with a magnitude of 5.6, a depth of 104 km, and geographic coordinates of 6.86° South Latitude and 107.01° East Longitude. The source mechanism analysis indicated a strike-slip movement for this earthquake. Numerous aftershocks followed, continuing until December 6, 2022, at 8:00 a.m. Monitoring reports documented a total of 390 aftershocks (BMKG, 2022). The earthquake caused extensive damage to buildings, and tragically, many lives were lost as a result of this disaster. The Cianjur earthquake is classified as a shallow crustal tectonic earthquake of the mainshock-aftershock type (Supendi et al, 2022).

Tectonic activity is responsible for altering the Earth's land surface through deformation. This deformation leads to the development of stress strains within the Earth's crust, indicating alterations in its dimensions (Janssen V, 2007). The primary cause of deformation in the Earth's crust or rocks is force, typically measured in terms of the force applied per unit area. Two important forces, tension (stress) and tensile stress (strain stress), exert their influence universally on the Earth's surface (Anderson, 2010). Deformation monitoring can be effectively conducted using GNSS (Global Navigation Satellite System). This technology provides valuable information regarding both vertical and horizontal deformation, but limited data and station observation (Gatsios et al, 2020, Hanif et al, 2023). In contrast, Sentinel-1 Synthetic Aperture Radar (SAR) technology offers the capability to map deformation across relatively extensive areas. It has found extensive applications in measuring deformation across various scenarios worldwide (Kusky, 2008).

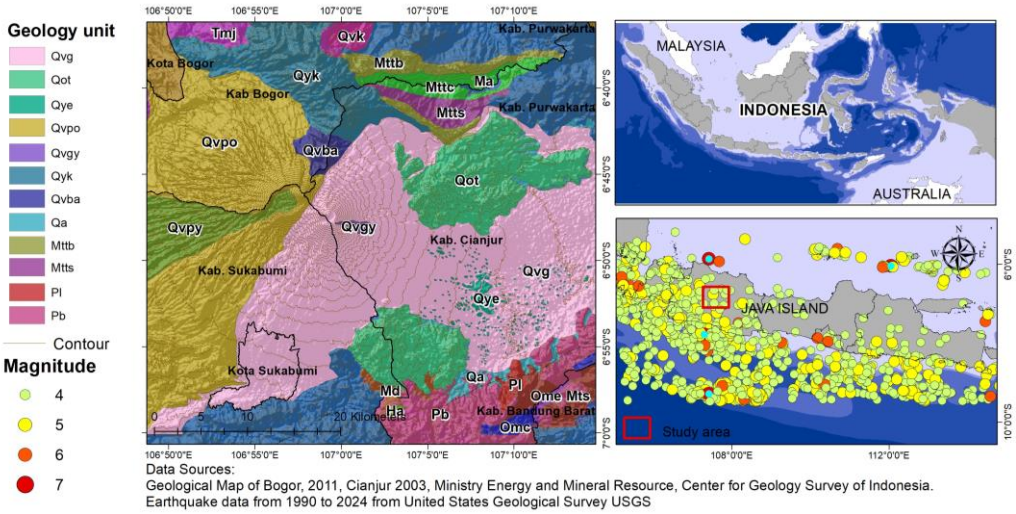

Figure 1. The geology map of studied area from and historical earthquakes above 4 M in the Java Island from 1990 to 2024 from USGS.

This research was conducted in the Cianjur Earthquake Area, situated in West Java Province on Java Island, Indonesia. The study area has been defined with a radius of 30 km from the epicenter of the earthquake. This region encompasses several districts, including Bandung Regency, Bandung City, Cianjur Regency, Sukabumi Regency, Sukabumi City, West Bandung Regency, and Purwakarta Regency, see Figure 1. The purpose of this research is to map and monitor the spatial distribution of crustal deformation, and assess deformation trends that occurred before and after the Cianjur earthquake in November 2022.

2. Materials and Methods

This research relies on data acquired from the Sentinel 1 SAR Earth observation satellite. These data are accessible free of charge through the Copernicus website https://dataspace.copernicus.eu/. The dataset includes information from specific dates: September 12, October 18, November 23, and December 5, 2022. Interferogram calculations were generated by comparing pairs of Sentinel-1 SAR satellite data, which served as the input for analyzing disparities between the two datasets. These calculations were meticulously examined using SNAP software. GNSS data were obtained from the Real-Time GNSS Observation Station operated by the Indonesia Geographical Information Agency (GNSS Data) from Badan Informasi Geospasial (BIG) Indonesia, with real-time data collected from September 8, 2022, to December 31, 2022.

2.1 DInSAR Analysis

Interferogram analysis is a technique employed to extract precise information about ground surface elevation at a pixel level. The Differential Interferometric Synthetic Aperture Radar (DInSAR) technique has proven highly effective with exceptionally accurate measurements down to the millimeter scale, offering a high level of spatial resolution (Razi et al, 2023). The process involves several critical stages, including interferogram formation, correction for topographic effects, filtering, and multi-search, followed by data unwrapping and displacement measurement.

Ground deformation monitoring, two sets of time-series data are employed (Krekes et al, 2020). Interferometry identifies two distinct phases, which contain valuable information about topographic profiles, variations in orbital paths, deformations, and phase noise, expressed as follows. The results of interferometric analysis yield Coherence and Phase values. The coherence value indicates the connection between two phase interferogram sheets, while the phase value is transformed into a displacement value (Razi et al, 2023, Hanif et al, 2024) following equation 1.

$$\varphi_1 = \frac{4\pi R}{\lambda} and\ \varphi_2 \frac{4\pi\ (R + \Delta R)}{\lambda} \qquad (1)$$
$$\Delta\varphi 1 = \varphi_1 - \varphi_2 = \frac{4\pi\ \Delta R}{\lambda}$$

Where φ_1 and φ_2 are satellite positions at different acquisition times, R is the slant range of the earth's surface to the satellite, and λ is radar wavelength. These two components contribute to the interferometric phase in InSAR processing. The basic deformation results obtained from InSAR were further refined by specifically considering various geographical phenomena factors to identify land surface deformation based on DInSAR, as illustrated in Equation 2.

$$\Delta\varphi 2 = \Delta\varphi_{flat} + \Delta\varphi_{height} + \Delta\varphi_{disp} + \Delta\varphi_{atm} + \Delta\varphi_{noise} \qquad (2)$$

Where $\Delta\ \varphi 2$ is the differential interferometric, $\Delta\varphi$ flat is the flat earth phase that presents in the interferometric phase, $\Delta\varphi$ height is a contribution of topographic in the

interferometric phase referred to as DEM, $\Delta\varphi$ disp is the relative displacement of the target T to the reference point, $\Delta\varphi$ atm is an interferometric phase that is introduced by an atmospheric condition, $\Delta\varphi$ noise is the noise introduced by temporal conditions, different look angles, or scatters.

The initial result of the D-InSAR analysis is a single image with ambiguous values in phase (π). The phase value resulting from interferometry is a single value represented in a visual grayscale, making it challenging to comprehend visually or numerically. Therefore, it requires an unwrapping process (Minh, et al. 2020). Coherence values range from 0 to 1, with values closer to 1 indicating better coherence and higher confidence in the interferometry results. This study uses a standard coherence threshold value of greater than 0.3 (Hongdong et al, 2011; Liu et al, 2021). With this coherence threshold, the displacement value is extracted based on reference to this coherence value.

2.1.1 Coordinate position movement

In this stage of tectonic plate deformation analysis, the Global Navigation Satellite System (GNSS) was employed, significantly enhancing this approach by providing extremely precise three-dimensional motion data for points in the vicinity of the volcano and beyond (Jerram, 2021). Over the past two decades, the widespread installation of GNSS Network stations has yielded a wealth of data that can be compiled to observe geodetic coordinate shift velocities, facilitating the monitoring of tectonic movements (Farofli et al, 2019).

In this research, GNSS data were collected from the Cianjur Station. The GNSS receivers used were of the LEICA GRX1200+GNSS type, compatible with the GPS-GLO satellite system, and equipped with LEIAR25 antennas. The GNSS Rinex data processing was conducted online using the AUSPOS Online GPS Processing Service, which leverages the resources of the Australian Government's International GNSS Service (IGS). The results of daily GNSS observations are presented in trend charts to observe the trend of daily deformation changes before and after the earthquake occurred.

3. Results and Discussion

The crustal deformation analysis unveiled a geological phenomenon of crustal deformation occurring between October 18, 2022, and November 23, 2022. These two sets of satellite image data were captured 35 days before and 1 day after the Cianjur earthquake. The results of the DInSAR analysis allowed for the determination of spatial displacement, ranging from -0.01 to 0.0014 cm. The vertical deformation exhibited minor changes, and even though these data span a relatively extensive time period, encompassing two days following the Cianjur earthquake, anomalous fluctuations in extreme deformation changes were not observed (see Figure 2). The conducted image enlargement at several specific locations showed displacements primarily ranging from yellow to blue, indicating values between 0.001 and -0.01 cm. Subsequently, interferometric analysis was conducted using data recorded on November 23, 2022, and December 5, 2022, with a time interval of 13 days.

The outcomes of this analysis revealed phase differences that led to displacement values, which are quite interesting to examine, as depicted in Figure 3. This image provides valuable insights into post-Cianjur earthquake displacement. Within approximately two weeks after the main earthquake, deformation in the form of uplift occurred, with displacement values ranging from 1.69 to 5.87 cm. This vertical deformation is particularly prominent in

several sub-districts that serve as research areas. The Pecet sub-district exhibits significant deformation, with most of it ranging from an uplift of 1.88 to 3.7 cm and an average uplift of 2.99 cm. Similarly, the nearby Cipanas sub-district experienced an average uplift of 2.88 cm. These areas are located in close proximity to the earthquake's epicenter, within a radius of only 15 km. Moving on to the Cianjur District predominantly witnessed uplift ranging from 1.7 to 3.8 cm, with an average of 2.94 cm. This sub-district is situated within a radius of 5 to 10 km from the epicenter of the earthquake, experiencing a substantial influence from the seismic pressure and turmoil.

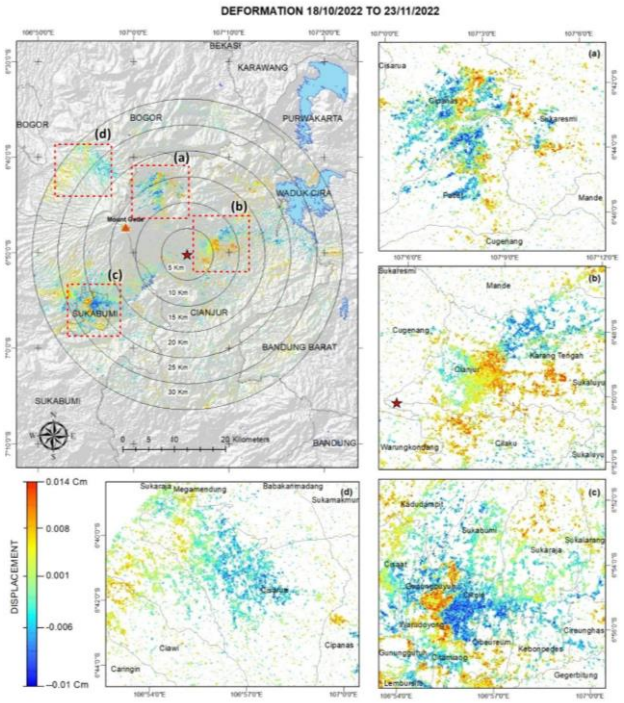

Figure 2. The ground deformation between 18 October 2022 to 23 November 2022

The most of the uplift ranged from 1.7 to 3.8 cm, with an average uplift of 2.69 cm. Only a few smaller spots experienced more significant uplift. This area includes sub-districts such as Cikole, Sukabumi, Gunungpuyuh, Warudoyong, and Citamiang, located within a radius of 20 to 25 km from the epicenter in the southwest region. The last figure, presents the Cisarua District, which lies within a radius of 25 to 30 km from the earthquake's epicenter, situated behind Mount Gede. In this district, deformation ranging from 1.8 to 3.7 cm occurred, with an average of 2.7 cm. These observations highlight the significant vertical displacement in various sub-districts within the affected area. The Cianjur sub-district, located within a radius of 5 to 10 km from the earthquake's epicenter, experienced extreme deformations as a direct consequence of tectonic activity. However, it's worth noting that buoyancy deformation also occurred in other areas, such as Cisarua, despite being farther from the earthquake's source. The degree of destruction in Cianjur was more severe due to its proximity to the epicenter, whereas Cisarua, with similar deformation values, was less impacted physically in terms of building damage.

The Cianjur area, reveals that this region had already experienced deformation in the month preceding the earthquake as depicted in Figures 2 and 3. Although the deformation during that period was not extensive, it was notable that the Cianjur area had a higher concentration of deformation centers between September 13, 2022, and October 18, 2022. During this time frame, when the earthquake occurred, this area experienced more significant buoyancy deformation.

The conditions of stress zones induced by this earthquake make them more susceptible to subsequent seismic events. This underscores the importance of understanding the geological and tectonic characteristics of specific areas in assessing earthquake risk and deformation potential, as referenced in Mulyaningsih's (2005) statement that weak zones experiencing deformation are more prone to repeat

deformation compared to zones that remain unaffected, even when they are in close proximity to the earthquake source.

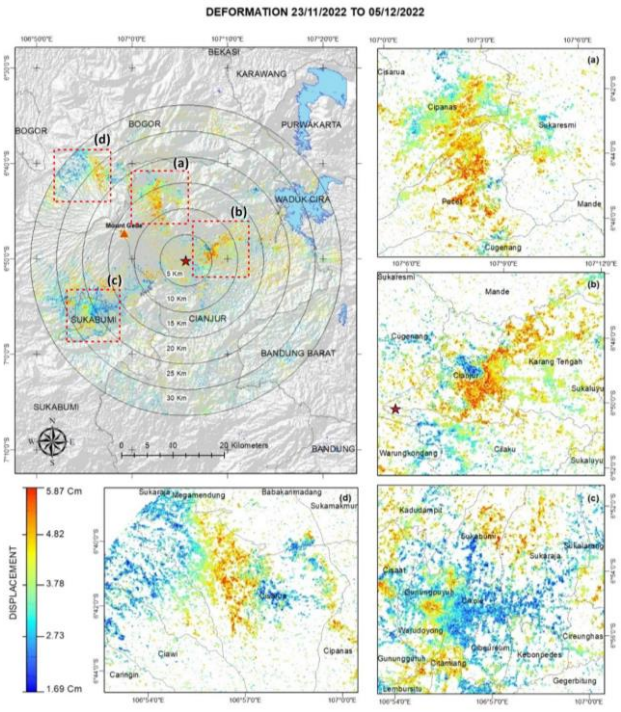

Figure 3. The ground deformation between 23 November 2022 to 05 December 2022.

The GNSS data collected from the Geospatial Information Agency were processed in the cloud using the AUSPOS online GNSS processing system. Coordinate information was extracted from GNSS data, revealing changes in horizontal positions. Notably, a significant deformation displacement of 12 cm to the east was detected at the Cianjur station. This substantial displacement indicates the direct impact of tectonic shifts during the earthquake period on the Cianjur station, which is situated in close proximity to the earthquake's epicenter. Further analysis of the GNSS observations reveals dynamic changes in vertical deformation over time. From October 18, 2022, to October 23, 2022, there was a decrease in height of -1.1 cm, signifying a subsidence trend. However, from October 23, 2022, to December 5, 2022, there was an increase in height, with values reaching up to 4.6 cm. These variations in vertical deformation reflect the complex and dynamic nature of the tectonic activity in the region during this period.

The results of vertical deformation measurements were visualized to track deformation trends at three specific observation times: before the earthquake, the day after the earthquake, and 13 days after the earthquake. These visualizations were created using both InSAR and GNSS data, as depicted in Figure 4. This approach allows for a comprehensive assessment of the changes in vertical deformation over this critical period, providing valuable insights into the impact of the earthquake and subsequent geological processes on the region.

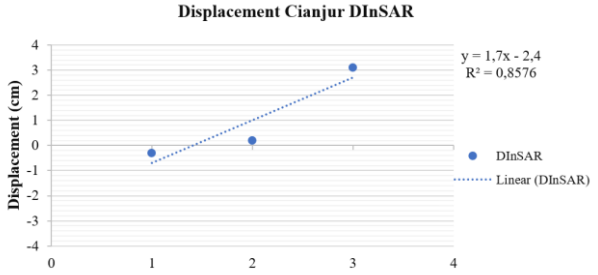

Figure 4. The deformation among 13/09/2022, 18/10/2022, 23/10/2022 and 05/12/2022, based on DInSAR

The image provides a clear depiction of the deformation trend before and after the tectonic earthquake. The linear trend line drawn from both DInSAR observations support the conclusion that the deformation at this location primarily takes the form of a buoyancy trend.

However, there are some distinctions in the information gathered from these two observation technologies. The GNSS results indicate that the ground surface at the observation station initially decreased in height and then experienced a significant uplift after

the earthquake, reaching 4.6 cm. This suggests a relatively rapid vertical displacement. However, the DInSAR analysis reveals a more gradual increase in deformation over the three observation periods. It starts from a value of -0.24 cm and ends at a height of 3.07 cm. This indicates a more continuous and progressively increasing vertical displacement, with a longer-term perspective provided by DInSAR. These differences in observations between GNSS and InSAR highlight the complementary nature of these techniques in capturing the complex nature of ground deformation in response to tectonic events. Together, they offer a more comprehensive understanding of the deformation processes occurring in the aftermath of the earthquake.

Indeed, it's entirely normal to observe differences in the results obtained from DInSAR and GNSS, as these are distinct technological tools employing different approaches to monitor ground deformation. However, despite these variations, the overarching conclusion remains consistent: both DInSAR and GNSS data indicate that there was a significant uplift in the Cianjur area following the tectonic earthquake that occurred in November 2022. This consensus on the occurrence of plate uplift underscores the reliability of multiple sources of data and adds credibility to the findings regarding the geological changes in the region.

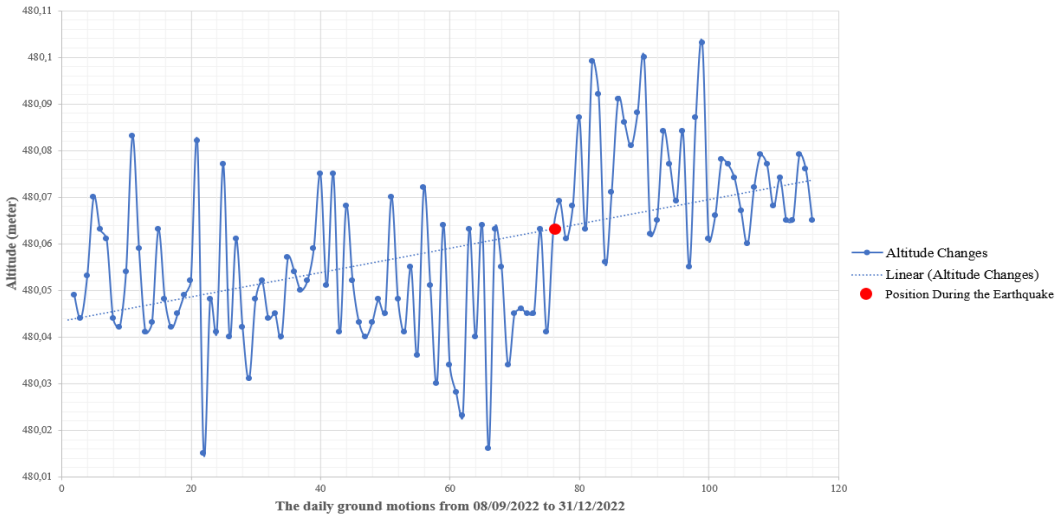

Figure 5. The ground motion before and after the Cianjur earthquake by GNSS observation.

Furthermore, the movement of the earth at the GNSS station in Cianjur was observed from November 8, 2022, to December 31, 2022. Valuable insights were obtained, specifically regarding the erosion and sinking of the tectonic plates in the Cianjur region. In Figure 5, the red dots represent the station's position at the time of the Cianjur earthquake. Before the Cianjur earthquake, it was known that there had been several instances of plate subsidence, but post-earthquake, the tectonic plates experienced an increasing trend of stress. This condition indicates this occurred downstream and approximately 20 days during co-seismic activity.

DInSAR and GNSS indeed employ different measurement principles, resulting in varying sensitivities when detecting deformation changes (Hastaoglu et al, 2023). DInSAR relies on radar satellite wave data to create interferogram maps, typically represented in pixel format. Conversely, GNSS utilizes navigation signals from multiple detected satellites as a reference to monitor position changes at specific observation station points (Farofli et al, 2019). Despite the differences in deformation measurements obtained from GNSS and InSAR, it's important to note that the assumption of minimal movement to address the ambiguity in InSAR changes is quite realistic (Komac et al, 2015; Susilo et al, 2023). This underscores one of the advantages of combining SAR and GNSS datasets: the information becomes more comprehensive compared to relying on a single deformation analysis (Soldato et al, 2021). Even if there are variations in the results of DInSAR and GNSS observations, these differences can be reconciled through consistent observations from both datasets (Franklin et al, 2018).

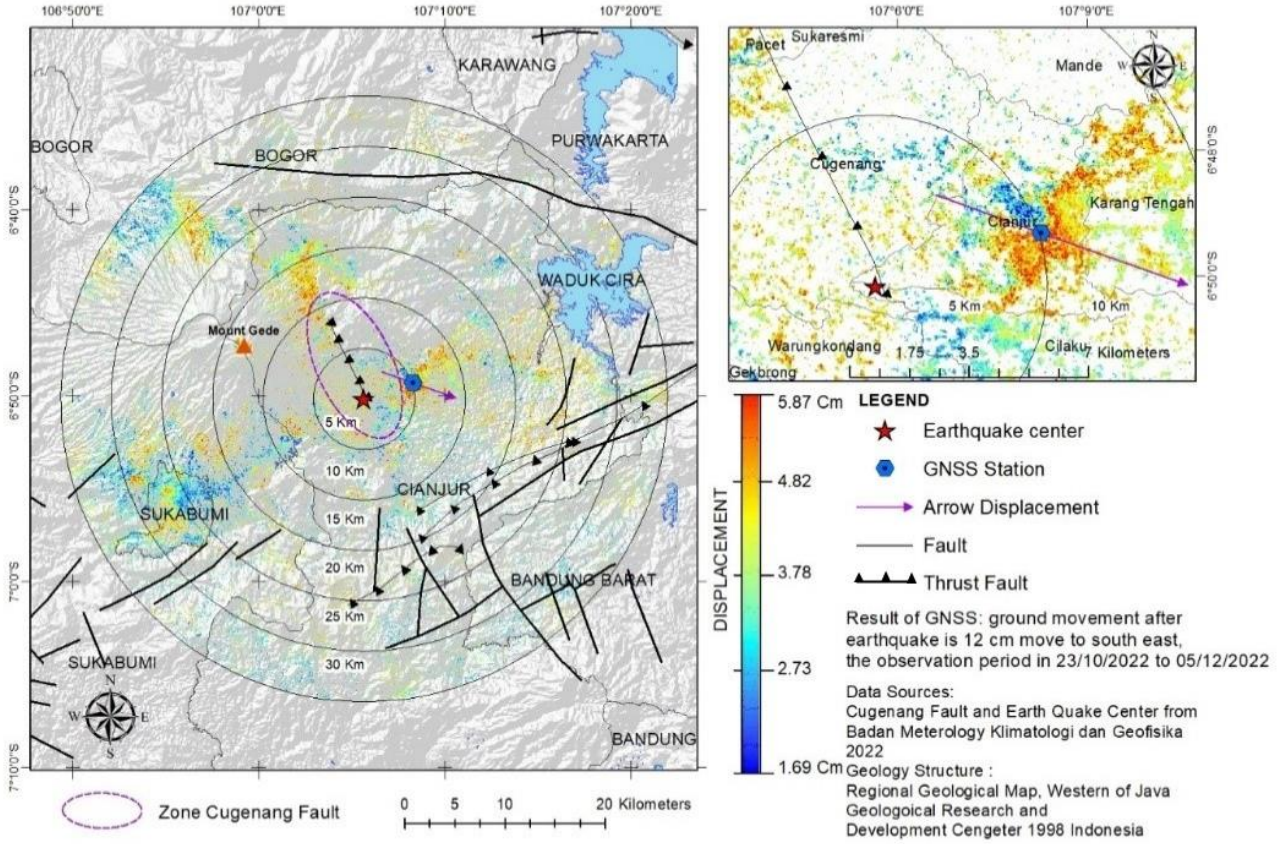

Figure 6. The vertical ground deformation movement results from DInSAR analysis and GNSS horizontal deformation direction.

Therefore, the slight disparities in the deformation results obtained from DInSAR and GNSS should be considered in context. Both methods offer distinct advantages, and the deformation information they provide is invaluable for gaining a deeper understanding

of tectonic deformation resulting from earthquakes. In the case of Cianjur, despite the variations in measurement results, both sources of information converge on the same conclusion: the occurrence of uplift. This alignment strengthens the overall assessment of the deformation process in the area, see Figure 6.

The map clearly illustrates the proximity of the earthquake source and the GNSS observation point, both located along the Cugenang fault line. The earthquake source is situated very near the deformed area in Cugenang and Cianjur subdistricts, within a radius of just 0 to 10 kilometers. This proximity implies that this region experienced direct effects from changes in land surface vibrations and stresses resulting from the earthquake. In terms of DInSAR observations during the period from October 23, 2022, to December 5, 2022, the maximum deformation detected in Cianjur subdistrict reached 3.8 cm. Additionally, the results of GNSS observations showed a position shift of up to 12 cm toward the southeast. These measurements indicate substantial ground displacement in response to the seismic activity. Then, in the Cugenang district, DInSAR observations revealed a maximum deformation of 5.8 cm, with an average deformation of 2.86 cm. This district, traversed by a fault line, experienced uplift and extreme vertical displacement attributed to the seismic activity and the movement of the Cugenang Fault.

These findings underscore the significant impact of tectonic events in the region, resulting in notable ground deformation and displacement along the fault line. The Cianjur earthquake and the Cugenang Fault are crucial in understanding the geological processes at play. The proximity of the earthquake epicenter and the Cugenang Fault supports the hypothesis that this earthquake was triggered by the displacement of the fault, resulting in various surface changes such as fractures and landslides.

The significant deformations observed are closely tied to the peak ground acceleration (PGA) experienced in the region's surface structures, including rocks and ground. The earthquake effects on ground vibrations are influenced by three primary factors: (a) the earthquake source, (b) the propagation path of seismic waves, and (c) local ground conditions (BMKG, 2022; Suspendi, 2022). It is known that the closer the earthquake source is, the stronger the ground vibrations tend to be. The thick layers of soft sedimentary soils can amplify and intensify surface vibrations.

The Cianjur earthquake is classified as a shallow-crust tectonic earthquake with a main shock followed by aftershocks. Notably, there was a distinct difference between the main shock, which occurred north of the, and the subsequent series of aftershocks that propagated northeastward from the main shock. This mechanical behavior is indicative of a left-lateral strike-slip movement from southwest to northeast (Natsuaki et al, 2022).

It is reasonable to assume that changes in the distribution of source positions between the main shock and aftershocks, driven by alterations in pressure and stress on the land surface, contributed to the observed changes in deformation values in Cianjur and Cugenang. This interpretation aligns with the results of the analysis conducted in this research, which indicate that significant deformations occurred, particularly in the vertical and horizontal dimensions, during the observation period following the main shock. These findings shed light on the dynamic and evolving nature of tectonic processes in the region.

4. Conclusions

Deformation monitoring data collected before and after the Cianjur tectonic earthquake, using InSAR and GNSS technology, have provided a comprehensive and detailed understanding of the spatial distribution representation. Meanwhile, a GNSS survey revealed vertical and horizontal deformation in the Cianjur Region. The vertical deformation trend is uplifted, and the larger vertical deformation observed is not caused by the main earthquake but by aftershocks. Apart from that, the horizontal deformation due to these aftershocks was quite large, with the tectonic movement reaching ±12 cm to the southeast. However, among the affected areas, Cugenang District recorded the most significant uplift a maximum of 5.8 cm because it was located at the epicenter of the earthquake. Our contribution from the results of this research highlights that the impact of co-seismic earthquake sources produces significant levels of vertical and horizontal deformation. This condition greatly influences ground stability, which is important as a consideration for updating the earthquake hazard map of the Cianjur area. This integrated approach has proven invaluable in understanding the complexity of ground deformation associated with seismic events. Areas that have been affected by deformation will be more vulnerable to future deformations because the instability of the land will easily experience destruction due to future earthquakes. For future work, we aim to assess the relationship between the stability of land slopes and SAR spectral response to further understand the to deformation that may occur. This will also involve exploring various variables with machine learning.

5. Acknowledgments

Acknowledgments to the College of Computing, Khon Kaen University, for providing a scholarship announced at No. 646/2022, to the primary author to complete the Master's degree study at the Department of Computer Science, Geoinformatics study program.

References

Anderson, S. R., Anderson P. S. 2010. Geomorphology the Mechanics and Chemistry Of Landscapes. *Published in the United Kingdom by Cambridge University Press*, UK. ISBN 978-0-521-51978-6 (pbk.)

BMKG. 2022. Ulasan Ground Motion dan Respon Spektra Gempa Bumi Cianjur 21 November 2022. Bidang Seismologi Teknik Badan Meteorologi Klimatologi dan Geofisika Published 6 December 2022. [online] https://www.bmkg.go.id/berita/.

Farolfi, G., Soldato, D.M., Bianchini, S., Casagli, N. 2019. A procedure to use GNSS data to calibrate satellite PSI data for the study of subsidence: an example from the north-western Adriatic coast (Italy). Taylor & Francis Online. *European Journal of Remote Sensing*. Volume 52, S4, 54-63. 10.1080/22797254.2019.1663710.

Franklin, K. R., and Huang, M. 2022. Revealing crustal deformation and strain rate in Taiwan using InSAR and GNSS. *Journal Geophysics*. Volume 49, no. 21, Nov. 2022, Art. 10.1029/2022GL101306.

Gatsios, T., Cigna, F., Tapete, D., Sakkas, V., Pavlou, K., Parcharidis, I. 2020. Copernicus Sentinel-1 MT-InSAR, GNSS and Seismic Monitoring of Deformation Patterns and Trends at the Methana Volcano, Greece. *Journal Apply Science*. Volume 10, 6445. 10.3390/app10186445.

Hanif, M., Apichontrakul, S. 2023. Vertical Ground Deformation Monitoring of the Sinabung Volcano in 2021-2022 using Sentinel-1 and DInSAR. *12th International Conference on Environmental Engineering, Science, and Management*. Pattaya Thailand. 18-RS-05, 304-311.

Hanif, M., Apichontrakul S., Razi. 2024. Multi-temporal InSAR analysis for monitoring the ground deformation of Mount Sinabung. *Preprint. Asia-Pacific Journal of Science and Technology*.

Hastaoglu, K.O., Poyraz, F., Erdogan, H. 2023. Determination of periodic deformation from InSAR results using the FFT time series analysis method in Gediz Graben. *Journal Natural Hazards*. Volume 117, 491–517. 10.1007/s11069-023-05870-w.

Hongdong, F., Kazhong D., Chengyu, J., Chuanguang, Z., Jiqun X. 2011. Land subsidence monitoring by D-InSAR technique. *Journal Mining Science and Technology (China*). Volume 21, 869–872. 10.1016/j.mstc.2011.05.030.

Janssen, V. 2007. Volcano deformation monitoring using GPS. *Journal of Spatial Science.* Volume 52: 1, 41-54, https://10.1080/14498596.2007.9635099.

Jerram Dougal. 2021. Introducing Volcanology a Guide to Hot Rock. Second Edition. Dunedin Academic Press Ltd, 8 Albany Street Edinburgh London. www.dunedinacademicpress.co.uk

Kerekes, A. H., Poszet, L. S., Baciu. 2020. Investigating land surface deformation using InSAR and GIS techniques in Cluj–Napoca city's most affected sector by urban sprawl (Romania*). Revista De Geomorfologie.* Volume 1, 43-59. 10.21094/rg.2020.097.

Kusky T. 2008. Volcanoes: Eruptions and Other Volcanic Hazards. *An imprint of Infobase Publishing*. 132 West 31st Street. New York NY 10001. ISBN: 978-0-8160-6463-2.

Komac, M., Holley, R., Mahapatra, P., Marel, D. V. H., Bavec, M. 2015. Coupling of GPS/GNSS and radar interferometric data for a 3D surface displacement monitoring of landslides. *Journal Landslides.* Volume 12, 241-257. 10.1007/s10346-014-0482-0.

Liu, G., Fu, H., Zhu, J., Wang, C., Xie, Q. 2021. Penetration Depth Inversion in Hyperarid Desert From L-Band InSAR Data Based on a Coherence Scattering Model. *IEEE Geoscience and Remote Sensing Letters*, Volume 18. 1981-1985. 10.1109/LGRS.2020.3011706.

Natsuaki, R., Hiroto, N., Naoya, T, Tadono, T. T. 2018. Sensitivity and Limitation in Damage Detection for Individual Buildings Using InSAR Coherence—A Case Study in 2016 Kumamoto Earthquake. *Journal Remote Sensing*. 10.3390/rs10020245.

Razi Pakhrur, JTS Sumantyo, Ming Yam Chua, Daniele Perissin, Takeo Tadono. 2023. Monitoring of tectonic deformation in the seismic gap of the Mentawai Islands using ALOS-1 and ALOS-2. *Journal Remote Sensing Applications: Society and Environment*. Volume 30. 1-15. 10.1016/j.rsase.2023.100973.

Susilo, S., Salman, R., Hermawan, W. 2023. GNSS land subsidence observations along the northern coastline of Java, Indonesia. *Journal Nature Scientific Data*. Volume 10, 421. https://doi.org/10.1038/s41597-023-02274-0.

Soldato Del Matteo, Pierluigi Confuorto, Silvia Bianchini, Paolo Sbarra and Nicola Casagli, 2021. Review of Works Combining GNSS and InSAR in Europe. *Journal Remote Sensing*. Volume 13, Is 9, 10.3390/rs13091684.

Saed, G. F. 2022. Earthquake-Induced Ground Deformation Assessment via Sentinel-1 Radar Aided at Darbandikhan Town. *Hindawi Journal of Sensors*., Volume 11. 10.1155/2022/2020069.

Supendi. P, Priyobudi. 2022. Analisis Gempabumi Cianjur (Jawa Barat) Mw 5.6 Tanggal 21 November 2022. https://prosesweb.bmkg.go.id/wp-content/uploads/Analisis-gempabumi-Cianjur_Supendi-dkk.-2022_rev-1.pdf.